ISSN 1063-7761, Journal of Experimental and Theoretical Physics, 2017, Vol. 124, No. 1, pp. 164–171. © Pleiades Publishing, Inc., 2017.
Original Russian Text © V.A. Kolpakov, S.V. Krichevskii, M.A. Markushin, 2017, published in Zhurnal Eksperimental'noi i Teoreticheskoi Fiziki, 2017, Vol. 151, No. 1, pp. 189–198.

STATISTICAL, NONLINEAR, AND SOFT MATTER PHYSICS

Kinetics of Charged Particles in a High-Voltage Gas Discharge in a Nonuniform Electrostatic Field

V. A. Kolpakov*, S. V. Krichevskii, and M. A. Markushin

Korolev Samara National Research University, Moskovskoe sh. 34, Samara, 443086 Russia

**e-mail: kolpakov683@gmail.com*

Received May 17, 2016

Abstract—A high-voltage gas discharge is of interest as a possible means of generating directed flows of low-temperature plasma in the off-electrode space distinguished by its original features [1–4]. We propose a model for calculating the trajectories of charges particles in a high-voltage gas discharge in nitrogen at a pressure of 0.15 Torr existing in a nonuniform electrostatic field and the strength of this field. Based on the results of our calculations, we supplement and refine the extensive experimental data concerning the investigation of such a discharge published in [1, 2, 5–8]; good agreement between the theory and experiment has been achieved. The discharge burning is initiated and maintained through bulk electron-impact ionization and ion–electron emission. We have determined the sizes of the cathode surface regions responsible for these processes, including the sizes of the axial zone involved in the discharge generation. The main effect determining the kinetics of charged particles consists in a sharp decrease in the strength of the field under consideration outside the interelectrode space, which allows a free motion of charges with specific energies and trajectories to be generated in it. The simulation results confirm that complex electrode systems that allow directed plasma flows to be generated at a discharge current of hundreds or thousands of milliamperes and a voltage on the electrodes of 0.3–1 kV can be implemented in practice [3, 9, 10].

DOI: 10.1134/S106377611613015X

1. INTRODUCTION

Investigating the kinetics of charged particles in gas discharges is of both fundamental and considerable practical interest in connection with their wide application for the generation of a low-temperature plasma used in various fields of science and engineering [11–19]. A low-temperature plasma is produced by gas discharges in the interelectrode space in a number of technological processes. In this case, the electrodes can be inside [20–22] or outside [15, 20, 23] the vacuum chamber containing a reactor. The authors of [1–4, 9, 10] proposed a new approach to the generation of a low-temperature plasma in the off-electrode space by a high-voltage discharge and substantiated the advantages of the off-electrode plasma over the low-temperature plasma generated by present-day technological processes.

These advantages are determined by the initiation and self-sustenance of a high-voltage gas discharge and the plasma flows generated by it on the straight segments of the field lines of a nonuniform electrostatic field [1, 2]. In [2] it was shown in that the presence of two oppositely directed flows of positively and negatively charged particles in the plasma generated by such a discharge provides a basis for its initiation and self-sustenance, while a model for the distribution of a nonuniform electrostatic field in the corresponding electrode system is presented in [4].

Therefore, gaining new knowledge about the behavior of charged particles in a high-voltage gas discharge existing in a nonuniform electrostatic field based on the available simulation results is of considerable interest.

The goal of this paper is to construct a model for calculating the trajectories of electrons, positive ions, and their energies by taking into account the collisions of these particles with gas molecules in a nonuniform electrostatic field and the strength of this field produced by the electrode system generating a high-voltage gas discharge.

This will allow the available theoretical knowledge about the processes in gas discharges existing in nonuniform electric fields to be expanded.

2. DESCRIPTION OF THE MODEL

The model of the electrostatic field produced by the system of electrodes generating a high-voltage gas discharge whose scheme is presented in Fig. 1 includes the equation [4]

$$z = x + iy = 2C \tanh\frac{\xi\pi}{2V} + \frac{h}{V}\xi. \qquad (1)$$

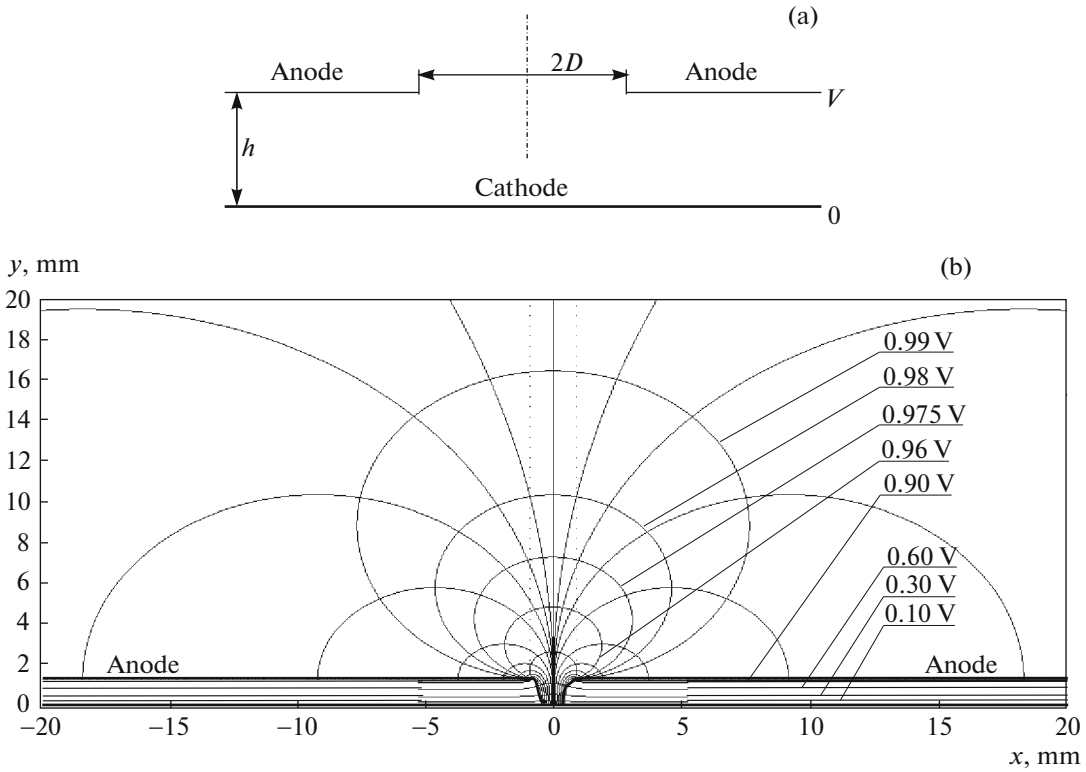

Fig. 1. (a) Scheme of the electrode system generating a high-voltage gas discharge and (b) the distribution of field and equipotential lines in such a system obtained using the system of equations (2) at $h = 1.2$ mm, $D = 0.9$ mm, and $V = 1200$ V.

Hence, by separating it into the real and imaginary parts, we obtain a system of parametric equations that allows the coordinates of the distribution of field and equipotential lines to be determined:

$$x = \frac{hu}{V} + 2C\frac{\sinh\frac{u\pi}{V}}{\cosh\frac{u\pi}{V} + \cos\frac{v\pi}{V}},$$
$$y = \frac{hu}{V} + 2C\frac{\sinh\frac{v\pi}{V}}{\cosh\frac{u\pi}{V} + \cos\frac{v\pi}{V}}. \quad (2)$$

Here, C is a constant coefficient dependent on the interelectrode spacing h and the radius D of the circular anode orifice, $\xi = u(x, y) + iv(x, y)$ is the complex potential of the electrostatic field in region z, and V is the voltage on the electrodes. We derived Eqs. (1) and (2) for the electrode system under consideration by the conformal mapping method based on the solution of the Schwarz–Christoffel integral. Such a configuration of electrodes and the discharge generated by it were considered in detail in [2–4].

In this paper Eqs. (1) and (2) are used to calculate the trajectories of electrons and positive ions in a high-voltage gas discharge existing in a nonuniform electrostatic field in the gas under consideration (nitrogen) and their energies by taking into account the collisions of these particles with gas molecules. In addition, such a calculation requires knowing the field strength distribution.

The electrostatic field strength is determined from the formula [24]

$$E = -i\frac{1}{z'(\xi)}. \quad (3)$$

Substituting Eq. (1) into (3) leads to an expression that allows the strength of the field under consideration at any point to be calculated from the known values of the functions $u(x, y)$ and $v(x, y)$:

$$E = -i\frac{V}{C\pi\left(1 - \tanh^2\frac{(u(x,y) - iv(x,y))\pi}{2V}\right) + h}. \quad (4)$$

When considering the trajectory of an electron in the above nonuniform electrostatic field, it is appropriate to divide it into separate segments with a step Δy on which the field will be assumed to be uniform. The coordinates of the initial point of the first segment are then (x_{e0}, y_{e0}), while the coordinates of the final points of such segments are represented as $(x_{en}, n\Delta y)$, where n is the ordinal number of the electron trajectory segment. The horizontal and vertical components of the initial and final electron velocities as well as the electrostatic field strength are represented on each seg-

ment in a similar way: $U_{ex(n-1)}$, $U_{ey(n-1)}$, U_{exn}, U_{eyn}, and $E_{x(n-1)}$, $E_{y(n-1)}$, respectively. We will assume that the motion of the electron begins from the point of its escape from the cathode surface with coordinates (x_{e0}, y_{e0}), which can be determined using the system of equations (2) by taking into account the fact that the cathode has zero potential and, consequently, $v = 0$:

$$x_{e0} = \frac{hu}{V} + 2C\frac{\sinh\frac{u\pi}{V}}{\cosh\frac{u\pi}{V}+1}, \qquad (5)$$
$$y_{e0} = 0.$$

Let the electron begin its motion with zero initial velocity ($U_{ex0} = 0$ and $U_{ey0} = 0$) along the straight segment of a field line, i.e., in a direction perpendicular to the cathode surface (see Fig. 1b), which allows the coordinates x of the initial and final points of the first segment to be considered identical ($x_{e0} = x_{e1}$). In this case, the electron is acted upon only by the imaginary component of the field strength determined from Eq. (4) provided that $v = 0$ and $u = \text{const}$.

Using the elementary formulas of classical physics concerning the calculation of the coordinates, velocity, and force acting on a charged particle in an electrostatic field and taking into account the above assumptions, we will write the expressions to determine the coordinates x_{en} and velocities of the electron at the end of each segment of its trajectory in a general form:

$$x_{en} = x_{e(n-1)} - U_{ex(n-1)}\frac{m_e\left(-U_{ey(n-1)} + \sqrt{U_{ey(n-1)}^2 - 2\frac{eE_{y(n-1)}}{m_e}\Delta y}\right)}{eE_{y(n-1)}}$$
$$-\frac{eE_{x(n-1)}}{2m_e}\left[\frac{m_e\left(-U_{ey(n-1)} + \sqrt{U_{ey(n-1)}^2 - 2\frac{eE_{y(n-1)}}{m_e}\Delta y}\right)}{-eE_{y(n-1)}}\right]^2, \qquad (6)$$

$$U_{exn} = U_{ex(n-1)} + \frac{E_{x(n-1)}}{E_{y(n-1)}}\left(-U_{ey(n-1)} + \sqrt{U_{ey(n-1)}^2 - 2\frac{eE_{y(n-1)}}{m_e}\Delta y}\right), \qquad (7)$$

$$U_{eyn} = \sqrt{U_{ey(n-1)}^2 - 2\frac{eE_{y(n-1)}}{m_e}\Delta y}. \qquad (8)$$

The corresponding values of u_n and v_n are found by substituting the coordinates x_{en} and $n\Delta y$ into system (2). The field strength on the segment with the coordinates of its initial and final points $(x_{en}, n\Delta y)$ and $(x_{e(n+1)}, (n+1)\Delta y)$ is calculated from Eq. (4) using these values. The calculations using Eqs. (2), (4), and (6)–(8) are performed each time until the length of the path traversed by the electron l_e becomes equal to the its mean free path λ_e dependent on the electron energy ε_e. On the whole, the iterations are continued until this condition holds. The energy of the electron on the traversed path is determined by the potential difference traversed by it. The equality $l_e = \lambda_e$ then specifies the coordinates of the point of interaction between the electron and a nitrogen molecule. The molecule is ionized by the electron if $\varepsilon_e \geq I$ (where I is the ionization energy of the nitrogen molecule, 15.6 eV [25]). Otherwise, an elastic interaction between these particles occurs. Analysis of the distribution of equipotential lines (see Fig. 1b) constructed using system (2) confirms the capability of the electron at the instant it exists from the anode orifice to ionize the N_2 molecule, because it has an energy greater than 790 eV (at voltage $V = 1200$ V on the electrodes), which exceeds I by an order of magnitude. Hence, when estimating the first electron mean free path, it is appropriate to use the ionization cross section σ_i in the calculations [25]. An electron in a strong field loses almost all of its energy due to its inelastic interaction [25]. Therefore, after each such collision it is necessary to check the condition $e\Delta V \geq I$, where $\Delta V = V - V_n$ is the potential difference accelerating this electron, and V_n is the field potential at the point of interaction [1]. If this condition is met, then λ_e is calculated in the order described previously; otherwise, the transport cross section for elastic interaction σ_{tr} should be used instead of σ_{tr} [26]. In that case, at $l_e = \lambda_e$ the electron energy losses through the corresponding collision are determined [27].

An inelastic collision of an electron with a nitrogen molecule gives rise to an additional electron and a positive ion. The trajectory of the newly formed electron is calculated according to the previously presented algorithm. In this case, the motion of such an electron

begins from the point at which the ionization of a residual-gas molecule with an initial velocity $U_e = (2(\varepsilon_e - I)/m_e)^{1/2}$ occurred and whose vector is aligned with the velocity vector of the electron that produced this ionization. In turn, a positive ion with an energy $\varepsilon'_{i0} = 3kT/2$ [27] begins to move along a field line toward the cathode, experiencing elastic collisions with residual-gas molecules and being scattered by them through a certain angle in each collision. According to [27, 28], the scattering angle of an ion after each collision with neutral particles is fairly difficult to estimate due to the dependence of this process on the impact parameter inaccessible to experimental determination. To simplify the problem, we assume that after the mth interaction the ion continues its motion along the same field line and reduce its multiple scatterings to its scattering as a result of the last collision preceding the ion–cathode collision. The coordinates of the points of such collisions are determined from the equality of the path l_i traversed by the positive ion and its mean free path λ_i dependent on the transport cross section for inelastic interaction $\sigma_{tr}(\varepsilon''_m)$, which was calculated from the formulas [26]

$$\sigma_{tr} = 2\sqrt{2}\pi a_0^2\sqrt{(\alpha/a_0^3)/(I_H/\varepsilon''_m)}, \quad (9)$$

$$\varepsilon''_m = \varepsilon_{im}\frac{m_i}{m_i + M}, \quad (10)$$

where $a_0 = 0.529 \times 10^{-8}$ cm is the Bohr radius, α is the polarizability of gas atoms and molecules in the ground state, $I_H = 13.6$ eV is the ionization potential of the hydrogen atom, ε''_m is the energy of the relative motion of the ion and molecule, and ε_{im} is the ion energy before each collision. Under the influence of a nonuniform electrostatic field generated by the electrode system (see Fig. 1), the ion moves along a field line, gaining an energy determined by the potential difference $\Delta V'$ traversed by it on its mean free path. Consequently, before each collision the ion will have an energy

$$\varepsilon_{im} = \varepsilon'_{i(m-1)} + e\Delta V'_m. \quad (11)$$

The energy of the ion after each collision, given the losses $\Delta\varepsilon_{im}$ that it experiences in elastic collisions, is then

$$\varepsilon'_{im} = \varepsilon_{im} - \Delta\varepsilon_{im}, \quad (12)$$

where

$$\Delta\varepsilon_{im} = \frac{2m_iM}{(m_i + M)^2}(\varepsilon_{im} - \varepsilon'_{i(m-1)})\ [27].$$

Given the energy of the ion at the instant of its scattering, we can determine its velocity $U_{i0} = (2\varepsilon'_{im}/m_i)^{1/2}$ using the formula for kinetic energy. This allows the components U_{ix0} and U_{iy0} of U_{i0} to be found at a specific scattering angle φ by determining the argument of the complex field strength $\arg(E)$ at the collision point:

$$U_{ix0} = U_i\cos(\arg(E) + \varphi), \quad (13)$$

$$U_{iy0} = U_i\sin(\arg(E) + \varphi). \quad (14)$$

The values of the components U_{ix0} and U_{iy0} are the initial ones for the subsequent calculation of the positive ion trajectory, which, as with the calculation of the electron trajectory, is divided into separate segments but now with a step Δx on which the field strength is assumed to be constant. This procedure is necessary, because the scattering of an ion through a certain angle suggests a deviation of its trajectory from the field line. The subsequent sequence of steps in calculating the ion trajectory is analogous to the sequence of steps for calculating the electron trajectory. Given the coordinates of the distribution of field lines, including the field line along which the ion under consideration moves, and the potential difference traversed by it from its formation to the scattering point with coordinates (x_{i0}, y_{i0}), we will calculate the field strength on the jth segment of the trajectory using Eq. (4). Thus, we will write the expressions to determine the coordinates y_{ij} and velocities of the ion at the end of the jth segment of its trajectory in a general form:

$$y_{ij} = y_{i(j-1)} + U_{iy(j-1)}t_{i(j-1)} + \frac{eE_{y(j-1)}}{2m_i}t^2_{i(j-1)}, \quad (15)$$

$$U_{ixj} = U_{ix(j-1)} + \frac{eE_{x(j-1)}}{m_i}t_{i(j-1)}, \quad (16)$$

$$U_{iyj} = U_{iy(j-1)} + \frac{eE_{y(j-1)}}{m_i}t_{i(j-1)}, \quad (17)$$

where

$$t_{i(j-1)} = \begin{cases} \dfrac{m_i\left(-U_{ix(j-1)} + \sqrt{U^2_{ix(j-1)} - 2\dfrac{eE_{x(j-1)}}{m_i}\Delta x}\right)}{eE_{x(j-1)}} \\ \text{for} \quad \Delta x > 0, \\ \dfrac{m_i\left(-U_{ix(j-1)} - \sqrt{U^2_{ix(j-1)} - 2\dfrac{eE_{x(j-1)}}{m_i}\Delta x}\right)}{eE_{x(j-1)}} \\ \text{for} \quad \Delta x < 0. \end{cases}$$

It should be noted that at $\Delta x > 0$ the calculation using these formulas is performed until the argument of the complex number $U_{ij} = U_{ixj} + iU_{iyj}$ is equal to $-\pi/2$, because the direction of the vector $\mathbf{U}_{ix}$ changes in this case and the ion is deflected from its previous direction under the electrostatic field. The subsequent calculation of the ion trajectory at $\Delta x < 0$ is performed until the arguments of U_{ij} and E_j are equal, which will suggests that the positive ion passed to a new field line.

By substituting the coordinates $x_{i(j-1)} + \Delta x, y_{ij}$ into system (2), we find the corresponding values of u_j and v_j using which the field strength on the segment bounded by the points with coordinates $(x_{i(j-1)} + \Delta x, y_{ij})$ and $(x_{ij} + \Delta x, y_{i(j+1)})$ is calculated from Eq. (4).

The calculations are performed using Eqs. (2), (4), and (9)–(17) until the ion collides with the cathode by taking into account the elastic losses of the ion through its collisions with residual-gas molecules executed when the condition $l_i = \lambda_i$ is met. If the energy ε_{im} with which the ion bombards the cathode is greater than the threshold one, i.e., $\varepsilon_{im} > \gamma\varepsilon_b$ (where ε_b is the sublimation energy of the cathode material atoms, which, for example, is 3.26 eV for aluminum [29]), then the sputtering of cathode material atoms begins [25] followed by the formation of etch pits on its surface [2].

3. RESULTS OF OUR CALCULATIONS

The calculations were performed at gas pressure $p = 0.15$ torr, temperature $T = 293$ K, voltage $V = 1200$ V on the electrodes, and constant $C = 0.12$ mm corresponding to the interelectrode spacing $h = 1.2$ mm and the anode orifice radius $D = 0.9$ mm [4]. The values of Δx and Δy were specified to be 0.5 mm. The full size of the computational domain was specified up to 20 mm along the x axis and up to 200 mm along the y axis. The number density of charged particles was taken to be $n_e \approx 3 \times 10^9$ cm^{-3} [1]; therefore, according to [30], the influence of the electric field produced by such particles on their trajectories may be disregarded in the calculations. As a result, using the model described above, we constructed the trajectories of electrons and positive ions in a high-voltage gas discharge in nitrogen existing in a nonuniform electrostatic field and the dependence of the field strength on the distance measured from the cathode surface in the direction of discharge propagation (along the y axis) (see Fig. 2).

Figure 2 presents the calculated dependence $E = f(y)$, from which it can be seen that the field strength E decreases sharply outside the electrodes ($y > 1.2$ mm) in the direction of discharge propagation from 400 V mm^{-1} in the anode orifice region to 1 V mm^{-1} at a distance of 13.5 mm from the anode. The strong nonuniform electrostatic field in the interelectrode space ($0 < y < 1.2$ mm) reaches 400–760 V mm^{-1}. The high field gradients accelerate the charged particles in the interelectrode space to significant velocities and generate a directed free motion of charges in the off-electrode space, determining their energy and trajectory. Our calculations confirm the corresponding qualitative estimates presented in several papers [1, 2, 5].

Analysis of the electron trajectories presented in Fig. 3a on an enlarged scale shows that leaving the cathode surface under the above electrostatic field

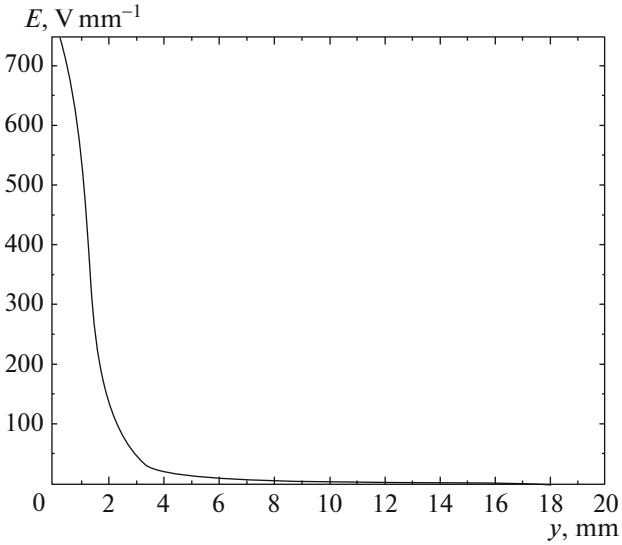

Fig. 2. Electrostatic field strength versus coordinate y along the anode orifice axis.

gradient, the electrons begin their motion in the interelectrode space along the straight segments of field lines. In this case, the length of the straight segments L increases in the direction from the anode orifice edge to the symmetry axis of the electrode system and changes parabolically in the range from 0.025 to 200 mm, respectively. Having a relatively small mass, the electrons acquire significant velocities (2.2×10^7 m s^{-1}) on their first mean free path λ_{e1}. Note that λ_{e1} for the electrons moving along the above trajectories is approximately the same, 14.25 mm. Because of inertia, the electrons tend to move in a straight line, which is why their trajectories do not coincide with the direction of propagation of the field lines when the latter deviate from rectilinearity. It follows from Fig. 3a and the corresponding results of our calculations that a maximum density of straight segments of field lines with a relatively large length is observed in region R of the symmetry axis of the electrode system with diameter $d_R = 100$ μm. It is in this region that the electron and ion trajectories coincide on lengths L comparable to or exceeding the sizes of the interelectrode space. Consequently, moving along the straight segments, most of the ions produced on such field lines reach the cathode at the point of electron escape, which is a necessary condition for the initiation and self-sustenance of a high-voltage gas discharge [5]. According to our calculations, at voltage $V = 1200$ eV on the electrodes the energy of the ions with which they bombard the cathode surface is ~1162.8 eV, a value sufficient for intense sputtering of its material and the emergence of ion–electron emission through which the discharge under consideration is maintained. The electrons leaving the cathode surface under the field gradient move along the trajectories presented in Fig. 3, gain-

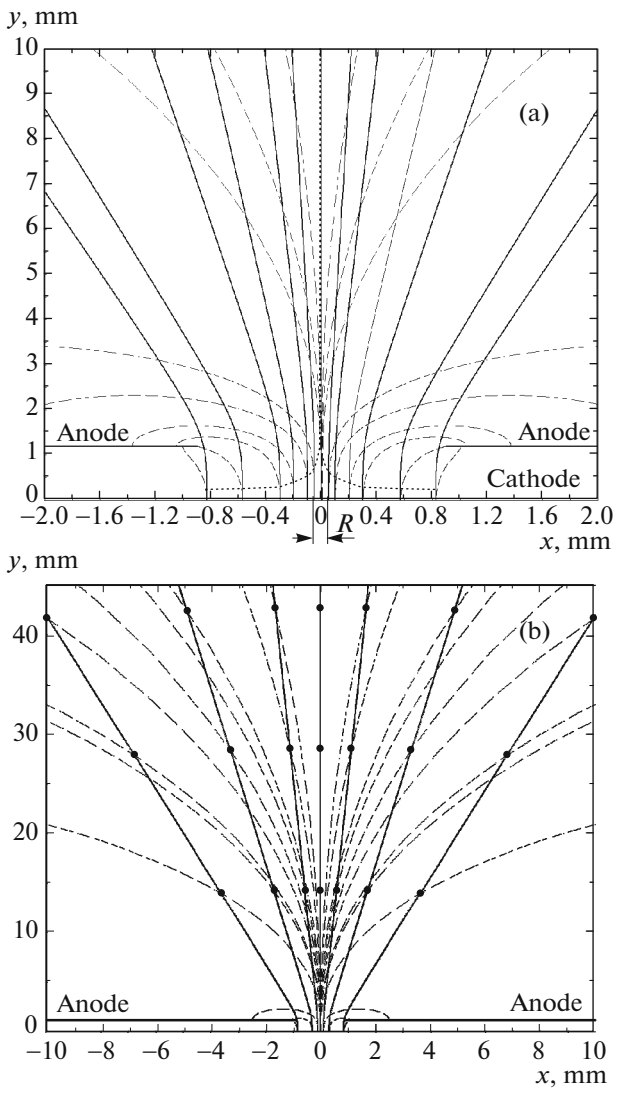

Fig. 3. Images of the electron trajectories (solid curves) and field lines (dashed curves) on an enlarged scale (a) and in the original form (b) (the filled circles indicate the points of ionization of the nitrogen molecule by the electron; the dashes indicate the boundary of the region where the electron trajectories coincide with the straight segments of the field lines).

ing an energy of ~1186.7 eV on the their first mean free path sufficient for the ionization of residual-gas molecules and the production of positive ions. The diameter of this cathode region is 1.66 mm at an anode orifice diameter of 1.8 mm, which determines the bulk electron-impact ionization boundaries. The electrons produced by ionization begin to move with velocities whose vectors are aligned with the velocity vectors of the electrons producing this ionization (see Fig. 3b), in good agreement with the conclusions reached in [27]. The bulk electron-impact ionization events occur along such trajectories provided that the electron energy is greater than or equal to the ionization energy. In turn, the electrons that lost almost all of their energy through their inelastic interaction subsequently experience elastic collisions and are not involved in the residual-gas ionization; therefore, their trajectories are not considered. Nevertheless, the proposed model allows the trajectories of such electrons to be calculated.

According to our calculations, the ion produced by the electron that left the cathode surface at x = 0.83 mm moves along a field line corresponding to the axial zone of the cathode surface toward the cathode (see Fig. 4, segment *a*) and experiences up to 13 collisions with nitrogen molecules before interacting with it. Thereafter, in accordance with the assumptions made when constructing the model, such an ion, because of its elastic collision with a molecule, is scattered through some angle φ and continues its motion along a trajectory different from the initial one, changing its direction (see Fig. 4, segment *b*). Acting on the ion, the force governed by the electrostatic field generated by the electrode system under consideration changes its trajectory and returns the ion to a different field line. In other words, the horizontal component of the ion velocity vector $\mathbf{U}_i$ rotates clockwise. The instant at which U_{ix} becomes zero suggests that the ion passes from segment *b* to segment *c* of the trajectory (see Fig. 4). In turn, segment *c* passes into a field line due to the influence of the field strength on the positive ion (see Fig. 4, segment *d*). The subsequent motion of the ion along this field line leads to its collision with the cathode and, as a consequence, to ion–electron emission. It should be noted that as the ion approaches the electrodes, its mean free path increases (see Fig. 4), suggesting an ion acceleration in this space due to the action of a high field gradient (see Fig. 2). This is typical of all the positive ions produced by bulk electron-impact ionization. As the length of the straight segment of a field line increases, the probability of scattering of the ions moving along this field line by residual-gas molecules decreases, their energy increases, and, consequently, the sputtering yield of cathode material surface atoms increases. As a result of such sputtering, an etch pit (zone C_{emis}) with a diameter of 300 μm containing region R with diameter $d_{R\text{exp}} \approx 100$ μm is formed on the cathode surface (see Fig. 5) [2]. Its presence is explained by the concentration of field lines with the largest lengths of the straight segments in it. The presented experimental data confirm that they are consistent with the results of our calculations ($d_{R\text{exp}} \approx dR$). The profile of such an etch pit (see Fig. 5b) corresponds to the previously described patterns of change in L and ion energy. According to the constructed model, a pit with a diameter of 300 μm on the cathode surface is obtained when the ion is scattered through an angle $\varphi \le 30°$. Consequently, the cathode surface regions with diameters of 300 and 100 μm determine the electron–ion emission boundaries and the axial zone involved in the discharge gen-

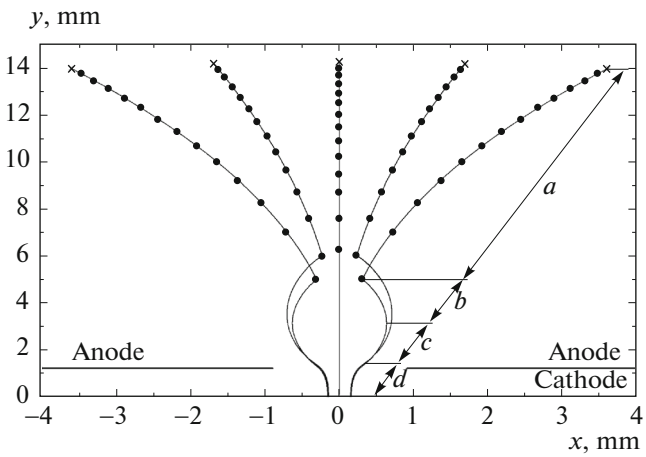

Fig. 4. Trajectories of positive ions (the cross indicates the points of ionization of the nitrogen molecule by the electron; the filled circles indicate the points of elastic interaction between the ion and nitrogen molecule).

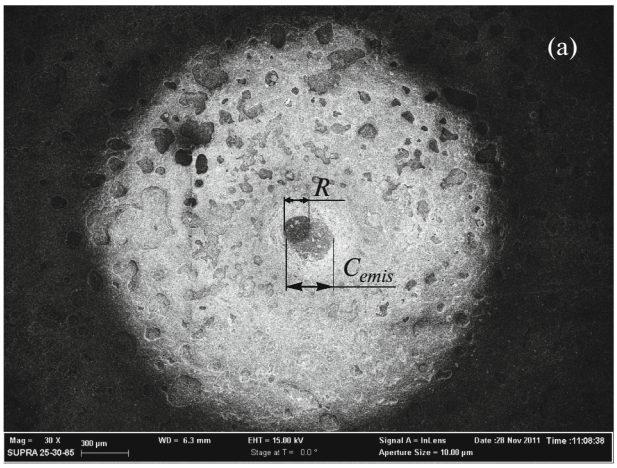

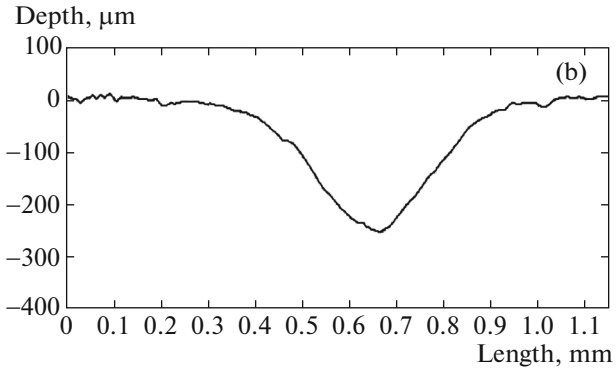

Fig. 5. (a) View of the cathode surface in the anode orifice region and (b) the profile of the etch pit on the cathode surface produced by positive ions.

eration. The results of our calculations are consistent with the results of our study of the current–voltage characteristic for the discharge under consideration. Using these results, it was experimentally established that the discharge is initiated and maintained through bulk electron-impact ionization and ion-electron emission at voltages on the electrodes $V \geq 1000$ V [1].

Thus, the proposed model allows the behavior of charges particles in a high-voltage gas discharge in a nonuniform electrostatic field and the mechanisms for the initiation and self-sustenance of such a discharge to be explained qualitatively and quantitatively.

4. CONCLUSIONS

Using the developed model, for the first time we have performed detailed calculations of the trajectories of electrons and positive ions in a high-voltage gas discharge in nitrogen existing in a nonuniform electrostatic field and the strength of this field, which considerably supplement and refine the qualitative estimates presented in [5]. According to the results of our calculations, the field under consideration in the off-electrode space reaches a strength that is several orders of magnitude smaller than that between the electrodes (10^4 V cm^{-1}). This confirms the generation of a free motion of charges with specific energies and trajectories outside the interelectrode space. Because of this, based on their experimental studies, the authors of [1, 3] proposed a new approach to the generation of a low-temperature plasma in the off-electrode space by the above discharge.

The pattern of change in the lengths of the straight segments of field lines from the anode orifice edge to the symmetry axis of the electrode system (from 0.025 to 200 mm) was determined quantitatively at specified parameters and pressure. This allowed the sizes of the axial zone of the cathode surface involved in the discharge generation, within which the trajectories of electrons and positive ions coincide, to be refined compared to [5]. Using the calculated trajectories of charged particles, we determined the boundaries of the bulk electron-impact ionization and ion-electron emission through which the discharge burning is initiated and maintained. We established that the positive ions produced by bulk electron-impact ionization move along field lines corresponding to the axial zone of the cathode surface, gaining an energy sufficient for its sputtering.

The developed model allows the following:

– to analyze the influence of parameters of the electrode system generating a high-voltage gas discharge on the kinetics of charged particles in such a discharge;

– to refine the physical and mathematical models for the interaction of these particles with the surface presented in [1, 2, 6–8, 31, 32];

– to create a new class of gas-discharge devices generating wide flows of off-electrode plasma free from the shortcomings typical of traditional methods

and devices for the generation of a low-temperature plasma. Therefore, a logical continuation of our work is the construction of an analogous model for an electrode system consisting of a cathode and a grid anode that allows the plasma flows noted above to be produced.

On the whole, our results are good agreement with the results obtained previously in experiments to investigate the peculiarities of a high-voltage gas discharge [1, 5] and the off-electrode plasma generated by it [1, 2], which can be of interest in nanotechnology applications.

ACKNOWLEDGMENTS

We express our sincere gratitude to I.V. Vagner, E.I. Bolgov, V.F. Grakun, V.L. Gokhfeld, and V.A. Kudlai for their paper [5] that specified the direction within which we have been working for more than 25 years and without which this paper would not be published. This work was supported by grants from the President of the Russian Foundation for State Support of Young Russian Ph.D. Scientists (MD-5205.2016.9) and the Russian Foundation for Basic Research (project no. 16-07-00494 A)

REFERENCES

1. N. L. Kazanskii and V. A. Kolpakov, Formation of Optical Microrelief in Off-Electrode Plasma of High-Voltage Gas Discharge (Radio Svyaz', Moscow, 2009) [in Russian].
2. V. A. Kolpakov, A. I. Kolpakov, and V. V. Podlipnov, Tech. Phys. **58**, 505 (2013).
3. N. L. Kazanskiy, V. A. Kolpakov, and V. V. Podlipnov, Vacuum **101**, 291 (2014).
4. M. A. Markushin, V. A. Kolpakov, S. V. Krichevskii, and A. I. Kolpakov, Tech. Phys. **60**, 376 (2015).
5. I. V. Vagner, E. I. Bolgov, V. F. Grakun, et al., Sov. Tech. Phys. **19**, 1042 (1974).
6. V. A. Kolpakov, Russ. Microelectron. **31**, 366 (2002).
7. N. L. Kazanskii, A. I. Kolpakov, and V. A. Kolpakov, Russ. Microelectron. **33**, 169 (2004).
8. N. L. Kazanskii and V. A. Kolpakov, Tech. Phys. **54**, 1284 (2009).
9. V. A. Kolpakov, A. I. Kolpakov, and S. V. Krichevskii, Instrum. Exp. Tech. **57**, 147 (2014).
10. V. A. Kolpakov, A. I. Kolpakov, and S. V. Krichevskii, Instrum. Exp. Tech. **58**, 683 (2015).
11. V. I. Erofeev, *Principles Underlying the Development of High-Informative Models of Plasma Kinetics* (Sib. Otdel. RAN, Novosibirsk, 2013) [in Russian].
12. L. D. Tsendin, Phys. Usp. **53**, 133 (2010).
13. M. Capitelli, C. M. Ferreira, B. F. Gordiets, et al., *Plasma Kinetics in Atmospheric Gases* (Springer, Berlin, 2000).
14. N. L. Aleksandrov, S. V. Kindysheva, and I. V. Kochetov, Plasma Sources Sci. Technol. **23**, 015017 (2014).
15. A. A. Orlikovskii, K. V. Rudenko, and S. N. Averkin, High Energy Chem. **40**, 182 (2006).
16. A. A. Serdobintsev, A. G. Veselov, and O. A. Kiryasova, Semiconductors **42**, 486 (2008).
17. Qi Wang, Xiangke Wang, Zhifang Chai, et al., Chem. Soc. Rev. **42**, 8821 (2013).
18. V. A. Soifer, *Diffractive Nanophotonics* (CRC, London, 2014).
19. A. L. Aleksandrov and I. V. Schweigert, J. Exp. Theor. Phys. **110**, 845 (2010).
20. M. G. Putrya, *Plasma Methods of Three-Dimensional VLSI Structure Forming* (MIET, Moscow, 2005) [in Russian].
21. N. V. Gavrilov, A. S. Mamaev, S. A. Plotnikov, et al., Surf. Coat. Technol. **204**, 4018 (2010).
22. X. L. Deng, A. Yu. Nikiforov, P. Vanraes, et al., J. Appl. Phys. **113**, 023305 (2013).
23. A. Y. Kovalgin, A. Boogaard, I. Brunets, et al., Surf. Coat. Technol. **201**, 8849 (2007).
24. N. N. Mirolyubov, M. V. Kostenko, M. L. Levinshtein, et al., *Calculation Methods of Electrostatic Fields* (Vyssh. Shkola, Moscow, 1963) [in Russian].
25. A. A. Kudryavtsev, A. S. Smirnov, and L. D. Tsendin, *Physics of Glow Discharge* (Lan', St. Peterburg, 2010) [in Russian].
26. E. D. Lozanskii and O. B. Firsov, *The Theory of the Spark* (Atomizdat, Moscow, 1975) [in Russian].
27. Yu. P. Raizer, *Gas Discharge Physics* (Springer, Berlin, 1991; Nauka, Moscow, 1992).
28. L. A. Artsimovich and S. Yu. Luk'yanov, *Motion of Charged Particles in Electric and Magnetic Fields* (Nauka, Moscow, 1972; Mir, Moscow, 1980).
29. V. A. Nikonenko, *Mathematic Simulation of Technological Processes* (MISiS, Moscow, 2001) [in Russian].
30. L. A. Artsimovich, *Elementary Plasma Physics* (Moscow, Atomizdat, 1963; Blaisdell, New York, 1965).
31. V. A. Kolpakov, Fiz. Khim. Obrab. Mater., No. 5, 41 (2006).
32. V. A. Kolpakov, Fiz. Khim. Obrab. Mater., No. 1, 53 (2007).

Translated by V. Astakhov